Popular Summary

Airborne Lidar Measurements of Aerosol Optical Properties During SAFARI-2000

M.J. McGill, D.L. Hlavka, W.D. Hart, E.J. Welton, and J.R. Campbell

The Southern African Regional Science Initiative (SAFARI) conducted during August-September 2000 provided a unique opportunity to study the climatology of southern Africa. Particular emphasis was placed on measurements of biomass burning and regional emissions. Measurement capabilities included ground-based, airborne, and spaceborne instrumentation from active, passive, and in situ sensors. Data from the multiple platforms and sensors will be used to better understand linkages between the land-atmosphere processes that are unique to southern Africa.

The Cloud Physics Lidar (CPL) onboard the high-altitude ER-2 aircraft provided data on cloud height and structure as well as aerosol and smoke plume structure, and optical depth. The spatial coverage attainable by the ER-2 permits studies of aerosol properties across wide regions of the southern African continent. As a result, the CPL measurements provide large-scale aerosol mapping that will be useful in studies of aerosol transport. During the SAFARI mission the CPL also provided measurements of boudary layer structure and optical properties to aid in studies of biomass burning.

This paper presents results of the CPL measurements from the SAFARI field campaign. Large-scale mapping of aerosols in the planetary boundary layer provides a regional climatology of aerosol distribution. Retrieved optical depth estimates are shown to be consistent with expectations and characteristics of regional variability are investigated. Comparisons of CPL-derived aerosol extinction profiles are shown to compare favorably with those from ground-based lidar instruments.

Airborne Lidar Measurements of Aerosol Optical Properties During SAFARI-2000

Dr. Matthew J. McGill
NASA Goddard Space Flight Center, Code 912
Greenbelt, MD 20771
phone: 301-614-6281
fax: 301-614-5492
email: mcgill@virl.gsfc.nasa.gov

Mr. Dennis L. Hlavka
Science Systems and Applications, Inc.
NASA Goddard Space Flight Center, Code 912
Greenbelt, MD 20771
phone: 301-614-6278
fax: 301-614-5492
email: sgdlh@virl.gsfc.nasa.gov

Mr. William D. Hart
Science Systems and Applications, Inc.
NASA Goddard Space Flight Center, Code 912
Greenbelt, MD 20771
phone: 301-614-6272
fax: 301-614-5492
email: billhart@virl.gsfc.nasa.gov

Dr. Evil J. Welton
Goddard Earth Sciences and Technology Center
NASA Goddard Space Flight Center, Code 912
Greenbelt, MD 20771
phone: 301-614-6279
fax: 301-614-5492
email: welton@virl.gsfc.nasa.gov

Mr. James R. Campbell
Science Systems and Applications, Inc.
NASA Goddard Space Flight Center, Code 912
Greenbelt, MD 20771
phone: 301-614-6273
fax: 301-614-5492
email: campbell@virl.gsfc.nasa.gov

submitted to Journal of Geophysical Research
SAFARI-2000 Special Issue

March 25, 2002

Abstract

The Cloud Physics Lidar (CPL) operated onboard the NASA ER-2 high altitude aircraft during the SAFARI-2000 field campaign. The CPL provided high spatial resolution measurements of aerosol optical properties at both 1064 nm and 532 nm. We present here results of planetary boundary layer (PBL) aerosol optical depth analysis and profiles of aerosol extinction. Variation of optical depth and extinction are examined as a function of regional location. The wide-scale aerosol mapping obtained by the CPL is a unique data set that will aid in future studies of aerosol transport. Comparisons between the airborne CPL and ground-based MicroPulse Lidar Network (MPL-Net) sites are shown to have good agreement.

Introduction

The Southern African Regional Science Initiative (SAFARI) during August-September 2000 provided a unique opportunity to study the climatology of southern Africa.[Swap *et al.*, 1988; Swap *et al.*, 2002] Particular emphasis was placed on measurements of biomass burning and regional emissions. Measurement capabilities included ground-based, airborne, and spaceborne instrumentation from active, passive, and in situ sensors. Data from the multiple platforms and sensors will be used to better understand linkages between the land-atmosphere processes that are unique to southern Africa.[Swap *et al.*, 2002]

During the SAFARI campaign a high priority was placed on airborne remote sensing measurements from the NASA ER-2 high altitude aircraft.[King *et al.*, this issue] The SAFARI field campaign was the first field deployment for the new ER-2 Cloud Physics Lidar (CPL). The CPL provided data on cloud height and structure as well as aerosol and smoke plume structure, and optical depth. Lidar profiling from the ER-2 nearly mimics spaceborne measurements, and the spatial coverage attainable by the ER-2 permits studies of aerosol properties across wide regions of the southern African continent. The large-scale aerosol mapping provided by the CPL will enhance studies of aerosol transport.

The CPL is designed to operate simultaneously at 3 wavelengths: 1064, 532, and 355 nm. However, for the SAFARI campaign the 355 nm channel was not yet operational. Vertical resolution of the CPL measurements is fixed at 30 m. Horizontal resolution is 1/10 second (~20 m at typical ER-2 speeds), but data are averaged to 1 second for the final data products. Primary data products include: time-height cross-section images; cloud and aerosol layer boundaries; optical depth for clouds, aerosol layers, and PBL; and extinction profiles. All data products are produced for both 532 and 1064 nm. A detailed description of the CPL instrument is beyond the scope of this paper, but details can be found in McGill *et al.* [2002].

During the SAFARI campaign 19 ER-2 flights were conducted, totaling nearly 120 flight hours. In this paper we present selected results from the CPL measurements. A composite of the derived optical depth of the

planetary boundary layer (PBL), along with statistics on the optical depth and aerosol extinction form the basis for this work. Comparisons between data from the CPL and ground-based Micro-Pulse Lidars (MPL) in the Micro-Pulse Lidar Network (MPL-Net) [Welton *et al.*, 2001] were made to validate the accuracy of the lidar results. One MPL was located in the Skukuza National Park in South Africa, the other in Mongu, Zambia. MPL-Net sites are co-located with Aerosol Robotic Network (AERONET) sunphotometers, and each site provides aerosol and cloud layer heights, and profiles of extinction and optical depth for each layer. Campbell *et al.* [this issue] discuss the MPL-Net results from SAFARI in more detail.

CPL Optical Analysis Procedures

To obtain cloud or aerosol optical depth from airborne lidar data requires two primary assumptions regarding the scattering characteristics of the particulates. The first assumption is that multiple scattering can be reliably quantified or neglected. For the CPL instrument multiple scattering is small due to the narrow field of view of the receiver (100 μradians, full angle) and is ignored. The second assumption is that the value of the extinction-to-backscatter ratio, or S-ratio, is known. The S-ratio is the total scattered and absorbed energy divided by the amount of backscattered energy, or 4π times the inverse of the product of the single-scattering albedo times the scattering phase function evaluated at a 180-degree scattering angle. For a given scattering layer the S-ratio is assumed to be constant. Under certain favorable circumstances the S-ratio can be estimated from the lidar data, but computations for the CPL data often will require externally computed values.

The goal of the optical properties analysis of the CPL lidar signal is to obtain particulate extinction cross section profiles (σ_P) and particulate layer optical depths (τ_P). The discussion given below essentially restates a derivation given many times in the literature (see, for example, Spinhirne *et al.*, 1996) and only an overview will be provided here.

The working lidar equation for a nadir pointing lidar can be written as:

$$P(z) = \left(\beta_p(z) + \beta_m(z)\right) T_p^2(z)\, T_m^2(z) \qquad \text{(Eqn. 1)}$$

where P(z) is the calibrated normalized lidar signal or attenuated backscatter coefficient. The total (particulate and molecular) volumetric backscatter coefficient at distance z is denoted by $\beta(z)$ and the two-way particulate and molecular transmission factor from the aircraft altitude to altitude z is given by $T^2(z)$. The two-way transmission is also expressed as $\exp[-2(\tau_m(z) + \tau_p(z))]$, where τ is optical depth and the subscripts m and p designate molecular and particulate contributions, respectively. Because the molecular contribution to the total backscatter and transmission can be computed from theory, Eqn. 1 is written with the molecular and particulate contributions explicitly separated.

The following relationships relate the two-way transmission to the S-ratio:

$$T_p^2 = e^{-2\int \sigma_p dz} \quad \text{and} \quad S_p = \frac{\sigma_p}{\beta_p} \text{ (assumed a constant for each layer), (Eqn. 2)}$$

and

$$T_m^2 = e^{-2\int \sigma_m dz} \quad \text{and} \quad S_m = \frac{\sigma_m}{\beta_m} \qquad \text{(Eqn. 3)}$$

where S_p and S_m are the effective particulate and molecular extinction-to-backscatter ratios, respectively. Rayleigh scattering theory can be used to calculate $T^2_m(z)$ if the vertical molecular density profile is accurately known (e.g., provided by sounding data). The molecular extinction-to-backscatter ratio, S_m is a constant $8\pi/3$ sr. The purpose of the CPL data processing is to solve for the vertical profiles of β_p. The true particulate optical depth and extinction profiles can be then be computed from the values of S_p and β_p.

Forward inversion processing continues throughout each particulate layer until $T_p(z) < T_L$ or until the signal from the earth's surface is detected, where T_L is a limit defined through error consideration. Extensive automated use of this algorithm has been incorporated into both the Global Backscatter Experiment (GLOBE) with aircraft lidar and analysis of ground-based MPL data from a 1998 field experiment at the Atmospheric Radiation Measurement (ARM) program site in Oklahoma.[Hlavka *et al.*, 1998] Backward inversion processing, where the boundary conditions are known at the base of the layer, is optionally used for low noise and high optical depth situations.

An important component of the transmission solution is the particulate S-ratio, S_p. When the particulate layer being analyzed is determined to meet the appropriate criteria for underlying signal analysis, an algorithm to calculate an estimate of S_p is used. Appropriate criteria include 1) layer is

optically thin with either a lower layer or earth's surface sensed and 2) enough clear air (no aerosols) exits below the layer to determine signal loss through the layer. The clear air zone must be at least a minimum thickness (around 0.6 km) and analysis is usually restricted to 3 km thickness. Ice clouds above 5 km are the most likely candidates for this analysis, although elevated aerosol layers with enough clean air below are also appropriate. Under these conditions, an estimate of $T_p(z)$ (and thus an estimate of effective optical depth for the layer) can be determined. A similar version of this analysis method has worked well during automated MPL data processing.[Welton *et al.*, 2002]

For atmospheric layers where S_p cannot be calculated, a value is assigned for each layer based on pre-defined look-up matrices of S_p, distinguishing between different cloud and aerosol regimes. Because the calculation of S_p requires a clear air zone below the layer, the PBL must always default to the pre-defined matrices unless the optical depth can be estimated from an independent instrument. Determination of S_p for aerosol (non-cloud) will be driven by geographic location, layer height, and relative humidity, with geographic location the most important factor. Geographic location can be divided into three main aerosol regimes: continental, desert, and maritime.[Ackermann, 1998; Welton *et al.*, 2000]

The CPL processing scheme first locates the top and bottom of every detectable layer at 1-second resolution and assigns it to be a cloud, elevated aerosol, or PBL. To calculate extinction and optical depth, an S-ratio must be

computed or assigned for each layer. For clouds and elevated aerosol layers the preferred procedure is to calculate the S-ratio, provided the previously stated conditions are met. If conditions are not met, then a value is assigned from a look-up table. In the PBL an independent measure of the aerosol optical depth (from AERONET, MPL, or AATS-14) permits an S-ratio to be computed. Using an independently measured optical depth allows the lidar inversion to be constrained to match that value and allows an estimate of S_p to be calculated. If no independent estimate is available, then the CPL processing algorithm defaults to a look-up table based on climatology.

The tropospheric and PBL S-ratio default values are primarily formulated from a method developed by Ackermann [1988] that relates relative humidity to S-ratio in three geographic regions: maritime, continental, and desert. As stated previously, the CPL data alone does not permit a unqiue retrieval of S-ratios for optical processing of PBL layers. However, other instruments, such as AERONET sunphotometers, can provide optical depth measurements that can be used to constrain the lidar inversion and thereby permit computation of S-ratios from the lidar data. Enough overflights of AERONET sites will allow compilation of an S-ratio assignment matrix that can be used rather than defaulting to a generic look-up table. For an experiment like SAFARI where AERONET sites were frequently overflown, reasonably accurate optical depths will result.

PBL Optical Depth Measurements

A prime reason to use the ER-2 aircraft during SAFARI was to obtain measurements in widely varying regions of southern Africa. Figure 1 shows a composite of the PBL aerosol optical depth derived from the 1064 nm CPL measurements. Figure 2 shows the corresponding composite picture for the 532 nm measurements. For these composite images the 1-second data were averaged into 2 minute intervals. Data from 13 flights (August 22, 24, 25, 27, 29, 31 and September 1, 4, 6, 7, 11, 13, 14) are included in these images. Any areas where no PBL was detected (due, e.g., to clouds above or low signal) are not plotted.

From Figures 1 and 2 it is evident that different regions are generally associated with differing levels of PBL aerosol optical depth. To aid in understanding the various regions four sectors were defined, with each sector being generally associated with distinct land characterstics [Le Canut, *et al.*, 1996] and different levels of industrialization and/or biomass burning. Sector 1, off the east coast and including the Lowveld region, is a non-industrial, largely savanna region. Sector 2 includes the heavily industrialized Highveld region. Sector 3 is also industrialized and includes Zambia, where extensive biomass burning was occurring during the SAFARI campaign. Finally, sector 4 is characterized coastal, mostly non-industrialized, and some desert areas.

The four sectors, while only grossly defined, provide a means of characterizing the aerosol properties of different regions. To quantify the information contained in Figures 1 and 2, histograms of the PBL aerosol optical depth were generated for both 532 and 1064 nm in each sector. The

histograms are displayed in Figures 3 and 4. The histograms of 532 nm aerosol optical depth (Figure 3) show markedly different structure in each sector. Not surprisingly, sector 4, off the Namibian coast, has the lowest overall optical depth and also the smallest spread in distribution. Also not unexpected is the distribution of sector 3, which displays a large spread in derived optical depth as well as the highest peak value for the aerosol optical depth.

The histograms of 1064 nm aerosol optical depth (Figure 4) also exhibit different features in each sector. As with the 532 nm data, sector 3 again has the largest spread in derived values resulting from the overall increased level of pollution in that sector. Interestingly, sector 4 shows a greater relative spread in values than does the 532 nm data, and reasons for this are not completely certain. It can be speculated that sector 4 contains more airborne dust and sea salt from nearby desert and maritime regions and therefore the 1064 nm signal is affected more strongly than the 532 nm signal.

Aerosol Extinction Profile Measurements

In addition to the PBL aerosol optical depth it is useful to examine the CPL-derived aerosol extinction profiles in each sector. An average aerosol extinction profile was computed from the measurements in each sector, as shown in Figure 5. In all cases, only profiles with no cloud contamination were included in the averages. In sectors 2 and 3 the ground height was generally ~1 km.

The aerosol extinction at 532 nm in sectors 1-3 is greater than at 1064 nm at all altitudes because the aerosols are products of fresh biomass burning and industrial pollution, which consists largely of small particles. In each profile the peak value of extinction occurs within 1 km of the ground with an almost monotonic and roughly linear decrease to zero above that level. The behavior in sectors 1-3 may result from nearly point-source pollution being confined by a low-level inversion where it dissipates horizontally as it becomes slowly mixed into the larger-scale PBL. The flights generally took place in mid- to late-morning, which is the time when nocturnal inversions break down and the top of the PBL rises.

The aerosol extinction profiles in sector 4 exhibit distinctly different characteristics with two peaks: a sharp peak at ~400 m and a broad peak centered at ~4250 m. A nearly aerosol-free zone exists with a minimum at about 1400 m (see Figure 7). In the lower region the extinction coefficients for both 532 and 1064 nm are nearly the same, which is characteristic of the relatively large aerosol particles that exist in marine boundary layers. In the upper layer the 532 nm extinction is notably greater than at 1064 nm. The elevated layer was transported from the continent out over the ocean and is undoubtedly a mixture of smoke and dust. Presence of smoke in the elevated layer is not unexpected since the heaviest biomass burning was occurring in and to the north of Zambia (within sector 3). This agrees with Cahoon *et al.* [1992], who clearly shows the predominance of burning during the August-September period occurs, generally, north of 25 degrees south latitude.

Continuous time-height profiles of aerosol extinction can be derived from CPL data. Figure 6 shows an example from August 24, 2000 off the east coast of South Africa and over Inhaca Island. Note the elevated aerosol layer propagating from the Highveld region out over the Indian Ocean, and the distinct clear band between the elevated aerosol and the marine boundary layer. We note that of the instruments involved in SAFARI, only the two lidar instruments (CPL and MPL) have the capability to provide continuous range-resolved profiles of aerosol backscatter and extinction.

The CPL data can also be used to calculate the S-ratio in regions where there are elevated aerosol layers, as frequently occurs off the coast of Namibia.[Carlson and Prospero, 1972] Under such conditions direct retrievals of the S-ratio of elevated aerosol layers were occasionally calculated. A good example is a prolonged interval of the September 14 flight near the coast of Namibia. Figure 7 shows an image of the extinction retrievals plus a plot of the calculated S-ratio in the elevated aerosol layer. A fit to the S-ratios shows the values rising with time, starting near 40 sr and increasing toward 60 sr. S-ratio values between 40-60 sr are in good agreement with those tabulated by Ackerman [1998] and Voss *et al.* [2001] for smoke particles. Data is only available for the 532 nm channel due to the inherently weak 1064 backscatter in the clean air below the layer. In these particular examples the 1064 nm return is too weak to calculate signal loss through the layer.

Whenever the ER-2 aircraft overflew an AERONET sunphotometer site the CPL analysis could calculate an S-ratio for the PBL layer. Tabulation of the various AERONET sites across southern Africa allowed categorizations of the CPL-derived aerosol S-ratio by general type, as shown in the Table 1. The largest component of the aerosol loading was smoke particles, although dust and other pollutants also contribute. Smoke particles are small and this property is characterized by a large wavelength dependence on the S-ratio as the smoke loading becomes dominant. The 532 nm channel is attenuated much more quickly in smoke-filled PBLs compared to the 1064 nm channel. Smoke has only a small effect on the S-ratio at 1064 nm.

Comparisons with Other Instruments

At several times during the campaign the ER-2 was directed to overfly the MPL sites to allow calibration and comparison of the ground-based and airborne sensors. Figure 8 shows a comparison of extinction profiles derived from the CPL and MPL on August 29, 2000 over Skukuza. The CPL profile is a 30-second average while the MPL profile is a 30-minute average. In calculating the extinction profiles the S-ratio for the CPL 532 nm channel was calculated to be 46.5 sr while the MPL (operating at 523 nm) S-ratio calculations ranged from 49 to 85 sr for the three profiles shown in Figure 8. Both lidars used AERONET optical depth measurements [Holben, *et al.*, 1998] co-located near the MPL site to calculate the S-ratios. The PBL aerosol optical depth was estimated to be 0.21.

Agreement between the two lidars is excellent at altitudes above ~1 km. In the lowest km there is some divergence in the measurements. Closer examination showed that the divergence is due to sampling of different volumes in a PBL that was far from homogeneous. Also contributing to discrepancies at the lowest altitudes is the fact that the CPL profile is an average along ~6 km compared to the stationary MPL measurements. For this reason, MPL profiles are shown from one hour prior to the overflight, during the overflight, and one hour after the overflight. As can be seen, considerable variability occurs in the lowest km. The degree of variability should not be unexpected, as the measurements were made in the morning hours when extensive biomass burning was occurring.

Figure 9 shows a single CPL-MPL comparison at the Mongu site on September 1, 2000. For this example the S-ratio for the CPL was calculated to be 55.7 sr and the MPL S-ratio was calculated to be 88.1 sr. The optical depth was determined to be 0.70 during this intercomparison period. The agreement in this comparison is not as good as at Skukuza, and there are several reasons for the discrepancy. First, the overflight time was after sunset, so the AERONET optical depth has to be extrapolated from measurements made before sunset. Second, the same caveat applies as in Figure 8, that the CPL is a 30-second average along the ER-2 flight track whereas the MPL is a 30-minute average at a stationary location. And third, there is a slight wavelength difference between the CPL and MPL.

The primary point of interest between the Skukuza and Mongu comparisons, however, is to illustrate the large difference in PBL extinction profiles between the two sites. The extinction coefficients at the Mongu site are a factor 2-4 greater than at the Skukuza site. Again, this should not be surprising given the predominance of biomass burning at the lower-latitude Mongu site compared to Skukuza at that time of year.[Cahoon *et al.*, 1992] Also, note that the degree of vertical variability is greater for the Skukuza case than for Mongu. CPL measurements repeatedly revealed complex PBL vertical structure over Skukuza and the Lowveld region, whereas PBL structure in more northerly regions was more vertically homogeneous.

The Ames Airborne Tracking 14-channel Sunphotomer (AATS-14) onboard the University of Washington CV-580 aircraft was also used extensively to validate CPL and MPL measurements. The AATS-14 measures atmospheric transmission (and hence optical depth and extinction) in bands from 354 nm out to 1558 nm.[Schmid, *et al.*, 2000] The channels of interest to CPL are those at 525 nm and 1020 nm, close to the CPL wavelengths. In all cases there was good agreement between CPL and the AATS-14, although in many cases comparisons in the lowest km suffered from variability due to inhomogeneity and different sampling volumes. Comparisons of CPL and AATS-14 are treated extensively in a companion paper by Schmid *et al.* [this issue]. One of the CPL-AATS comparisons (Figure 9 in Schmid *et al.*) is taken over Inhaca Island on August 24, corresponding to time 8:10 UTC in Figure 6.

Conclusion

The SAFARI field campaign during August-September 2000 provided a unique opportunity to study the climatology of southern Africa. Remote sensing instruments onboard the NASA ER-2 high-altitude aircraft permitted measurements in widely varying regions with multiple sensors. The CPL was a new and unique instrument for the SAFARI campaign and provided high resolution profiles of cloud and aerosol structure. In particular, the CPL provided information on PBL optical properties and variability. As shown, the CPL can be used for wide-scale mapping of aerosol loading and these measurements will prove useful in aerosol transport studies. Among the instruments participating in SAFARI, the CPL was the only airborne instrument capable of providing continuous, range-resolved profiles of aerosol extinction. In addition, the CPL data reveal detailed vertical structure that was not available from other instruments.

Segregating the CPL measurements into sectors based on geography and degree of industrialization allows examination of aerosol properties by region. The PBL aerosol optical depth and the aerosol extinction profiles show the heaviest aerosol loading over the northern region (sector 3). Although the sectors used here were only grossly defined it is still possible to see different features in the different regions. Future work will focus on refining the sector definitions based on better knowledge of geographical and local emission considerations.

References

Ackermann, J., "The extinction-to-backscatter ratio of tropospheric aerosol: a numerical study," *Journal of Atmospheric and Oceanic Technology*, **15**, 1043-1050 (1998).

Cahoon, D.R., Jr., B.J. Stocks, J.S. Levine, W.R. Cofer, and K.P. O'Neill, "Seasonal distribution of African savanna fires," *Nature*, **359**, 812-815 (1992).

Campbell, J.R., et al., *Journal of Geophysical Research*, submitted.

Carlson, T.N., and J.M. Prospero, "The long-range movement of Saharan air outbreaks over the northern equatorial Atlantic," *Journal of Applied Meteorology*, **11**, 283-297 (1972).

Hlavka, D.L., J.D. Spinhirne, and J.R. Campbell, 1998: "Aerosol analysis techniques and results from micro pulse lidar," Proceedings of 19th International Laser Radar Conference, Annapolis, MD, July 6 – 10, 1998.

Holben, B.N., T.F. Eck, I. Slutsker, D. Tanre, J.P. Buis, A. Setzer, E. Vermote, J.A. Reagan, Y.J. Kaufman, T. Nakajima, F. Lavenu, I. Jankowiak, and A. Smirnov, "AERONET - A federated instrument network and data archive for aerosol characterization," *Rem. Sens. Environ.*, **66**, 1-16 (1998).

When elevated aerosol layers are present it is possible to estimate the S-ratio from CPL data. A case study using an elevated layer off the west coast of Namibia resulted in S-ratios between 40-60 sr at 532 nm, which is consistent with S-ratios expected for smoke. In non-elevated layers (e.g., PBL) it is not possible to uniquely calculate S-ratios from lidar data. However, optical depth measurements from AERONET or AATS-14 sunphotometers can be used to constrain the lidar inversion. In such cases, PBL S-ratios were calculated to be 42-72 sr at 532 nm and 32-35 sr at 1064 nm.

Comparison of CPL-derived aerosol extinction profiles with those derived from ground-based MPL systems shows good agreement. There is, however, some discrepancy in the lowest km. Detailed investigation revealed that the discrepancy is caused by aerosol inhomogeneity in the lowest levels of the PBL. Comparisons with the AATS-14 sunphotometer, shown in a companion paper, also show good agreement.

Acknowledgements

The Cloud Physics Lidar is sponsored by NASA's Earth Observing System (EOS) office and by NASA Radiation Sciences, Code YS. We also thank Dr. Beat Schmid of the Bay Area Environmental Research Institute for his efforts in comparing CPL and AATS-14 data, and Mr Brent Holben of AERONET for access to CIMEL sunphotometer data.

King, M.D., S. Platnick, and C.O. Moeller, "Remote sensing of smoke, land and clouds from the NASA ER-2 during SAFARI 2000," *Journal of Geophysical Research*, submitted (2002).

Le Canut, P., M.O. Andreae, G.W. Harris, F.G. Wienhold, and T. Zenker, "Airborne studies of emissions from savanna fires in southern Africa: 1. Aerosol emissions measured with a laser optical particle counter," *Journal of Geophysical Research*, **101**(D19), 23615-23630 (1996).

McGill, M.J., D.L. Hlavka, W.D. Hart, V.S. Scott, J.D. Spinhirne, and B. Schmid, "The Cloud Physics Lidar: instrument description and initial measurement results," *Applied Optics*, in press.

Schmid, B., J.M. Livingston, P.B. Russell, P.A. Durkee, H.H. Jonsson, D.R. Collins, R.C. Flagan, J.H. Seinfeld, S. Gasso, D.A. Hegg, E. Ostrom, K.J. Noone, E.J. Welton, K.J. Voss, H.R Gordon, P. Formenti, and M.O. Andreae, "Clear-sky studies of lower tropospheric aerosol and water vapor during ACE-2 using airborne sunphotomoeter, airborne in-situ, space-borne, and ground-based measurements," *Tellus B*, **52**, 568-593 (2000).

Schmid, B., J. Redemann, P.B. Russell, P.V. Hobbs, D.L. Hlavka, M.J. McGill, W.D. Hart, B.N. Holben, E.J. Welton, J. Campbell, O. Torres, R. Kahn, D. Diner, M. Helmlinger, D.A. Chu, C. Robles Gonzalez, and G. de Leeuw, "Coordinated airborne, spaceborne, and ground-based measurements of

massive, thick aerosol layers during the dry season in Southern Africa," *Journal of Geophysical Research*, submitted.

Spinhirne, J.D., W.D. Hart, and D.L. Hlavka, "Cirrus infrared parameters and shortwave reflectance relations from observations," *Journal of Atmospheric Science.*, **53**, 1438-1458 (1996).

Swap, B., J. Privette, M. King, D. Starr, T. Suttles, H. Annegarn, M. Scholes and C.O. Justice, "SAFARI 2000: a southern African regional science initiative," *EOS Earth Observer*, **10**(6), 25-28 (1998).

Swap, R.J., H.J. Annegarn, and L. Otter, "Southern African Regional Science Initiative (SAFARI 2000): condensed science plan," *South African Journal of Science*, submitted (2002).

Swap, R.J., H.J. Annegarn, J.T. Suttles, J. Haywood, M.C. Helmlinger, C. Hely, P.V. Hobbs, B. N. Holben, J. Ji, M. King, T. Landmann, W. Maenhaut, L. Otter, B. Pak, S. J. Piketh, S. Platnick, J. Privette, D. Roy, A.M. Thompson, D.Ward, R. Yokelson, "The Southern African Regional Science Initiative (SAFARI 2000) dry-season field campaign: an overview," *South African Journal of Science*, submitted (2002).

Voss, K.J., E.J. Welton, P.K. Quinn, J. Johnson, A. Thompson, and H. Gordon, "Lidar measurements during Aerosols99", *Journal of Geophysical Research*, **106**, 20821-20832 (2001).

Welton, E.J., K.J. Voss, H.R. Gordon, H. Maring, A. Smirnov, B. Holben, B. Schmid, J.M. Livingston, P.B. Russell, P.A. Durkee, P. Formenti, M.O. Andreae, "Ground-based lidar measurements of aerosols during ACE-2: inistrument description, results, and comparisons with other ground-based and airborne measurements", *Tellus B*, **52**, 635-650 (2000).

Welton, E.J., J.R. Campbell, J.D. Spinhirne, and V.S. Scott, "Global monitoring of clouds and aerosols using a network of micro-pulse lidar systems," in *Lidar Remote Sensing for Industry and Environmental Monitoring*, U. N. Singh, T. Itabe, N. Sugimoto, (eds.), *Proceeding of the SPIE*, **4153**, 151-158 (2001).

Welton, E.J., K.J. Voss, P.K. Quinn, P.J. Flatau, K. Markowicz, J.R. Campbell, J.D. Spinhirne, H.R. Gordon, and J.E. Johnson, "Measurements of aerosol vertical profiles and optical properties during INDOEX 1999 using micro-pulse lidars", *Journal of Geophysical Research*, in press (2002).

Table 1: CPL PBL S-ratio tendencies as a function of aerosol loading.

Aerosol Category	Average S-ratio 532 nm	Standard Deviation (532 nm)	Average S-ratio 1064 nm	Standard Deviation (1064 nm)	Number of Observations
Continental, with light aerosol	42.5 sr	7.6	31.9 sr	4.7	7
Continental, with moderate aerosol	53.0 sr	4.9	33.7 sr	2.7	8
Continental, with heavy aerosol	72.2 sr	2.0	35.4 sr	6.0	8

Figure Captions

Figure 1: Composite map of CPL-derived 1064 nm PBL aerosol optical depth. Aerosol optical depth magnitude is denoted by the color scale. Four sectors have been defined based on differing geographical and industrial characteristics (see text).

Figure 2: Same as Figure 1, but for 532 nm PBL aerosol optical depth. Note that the color scales differ between Figures 1 and 2.

Figure 3: Histograms of 532 nm PBL aerosol optical depth by sector as a percentage of total observations. Sector numbers correspond to those defined in Figures 1 and 2. Optical depth measurements are binned in 0.01 increments.

Figure 4: Same as Figure 3, except for 1064 nm PBL aerosol optical depth.

Figure 5: Average profiles of aerosol extinction by sector. Sector numbers correspond to those defined in Figures 1 and 2. In each panel the black line is 1064 nm extinction and the gray line is 532 nm extinction. Only profiles with no cloud contamination are included in the averages. The ground elevation in sectors 2 and 3 was generally ~1 km.

Figure 6: CPL data segment from August 24, 2000 showing elevated aerosol layer above west coast over Inhaca Island. (a) 1064 nm attenuated backscatter profiles; (b) 1064 nm extinction profiles; (c) 532 nm attenuated backscatter profiles; and (d) 532 nm extinction profiles.

Figure 7: Two-hour data segment from September 14, 2000 showing elevated aerosol layer off the west coast of Namibia. (a) 1064 nm attenuated backscatter profiles; (b) 532 nm attenuated backscatter profiles; (c) 532 nm extinction profiles; and (d) S-ratio of elevated aerosol layer derived from 532 nm data.

Figure 8: Comparison of extinction profiles from CPL and MPL on August 29, 2000 at Skukuza. CPL profile is a 30-second average. MPL profiles are 30-minute averages centered at the times listed. Differences in the lowest km are due to aerosol inhomogeneity during the measurements.

Figure 9: Comparison of extinction profiles from CPL and MPL on September 1, 2000 at Mongu, Zambia. Note difference in magnitude and vertical structure compared to Figure 8.

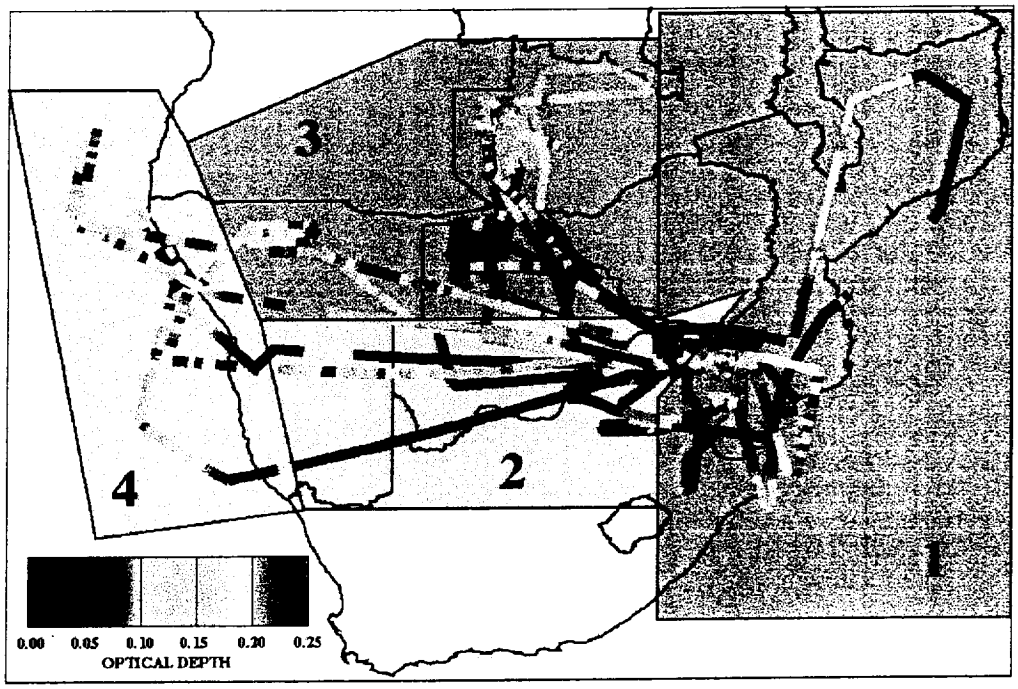

Figure 1: Composite map of CPL-derived 1064 nm PBL aerosol optical depth. Aerosol optical depth magnitude is denoted by the color scale. Four sectors have been defined based on differing geographical and industrial characteristics (see text).

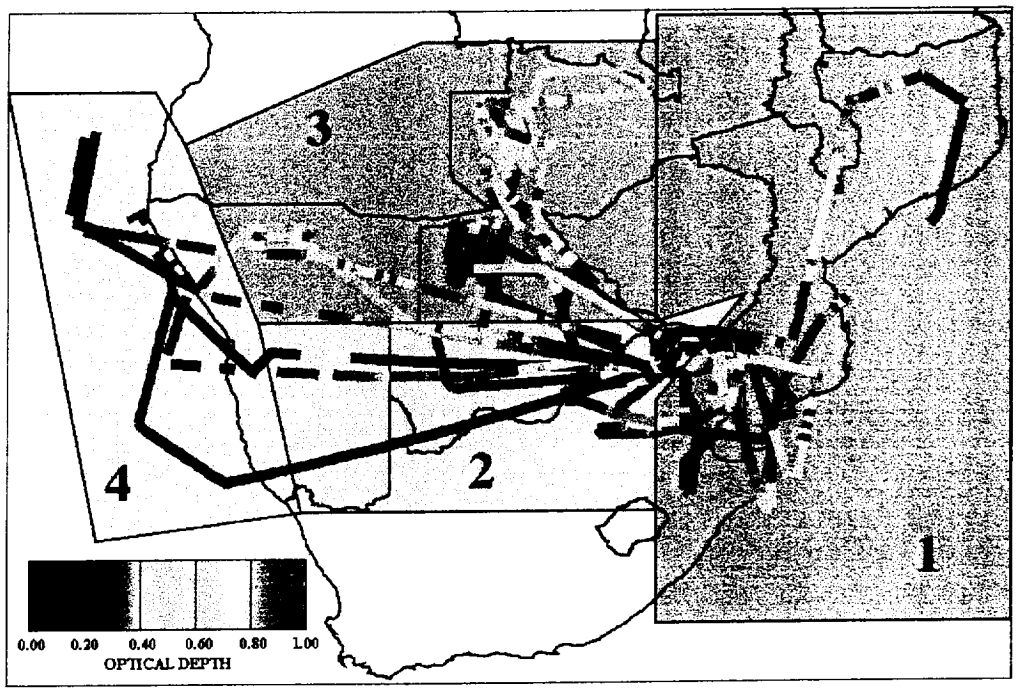

Figure 2: Same as Figure 1, but for 532 nm PBL aerosol optical depth. Note that the color scales differ between Figures 1 and 2.

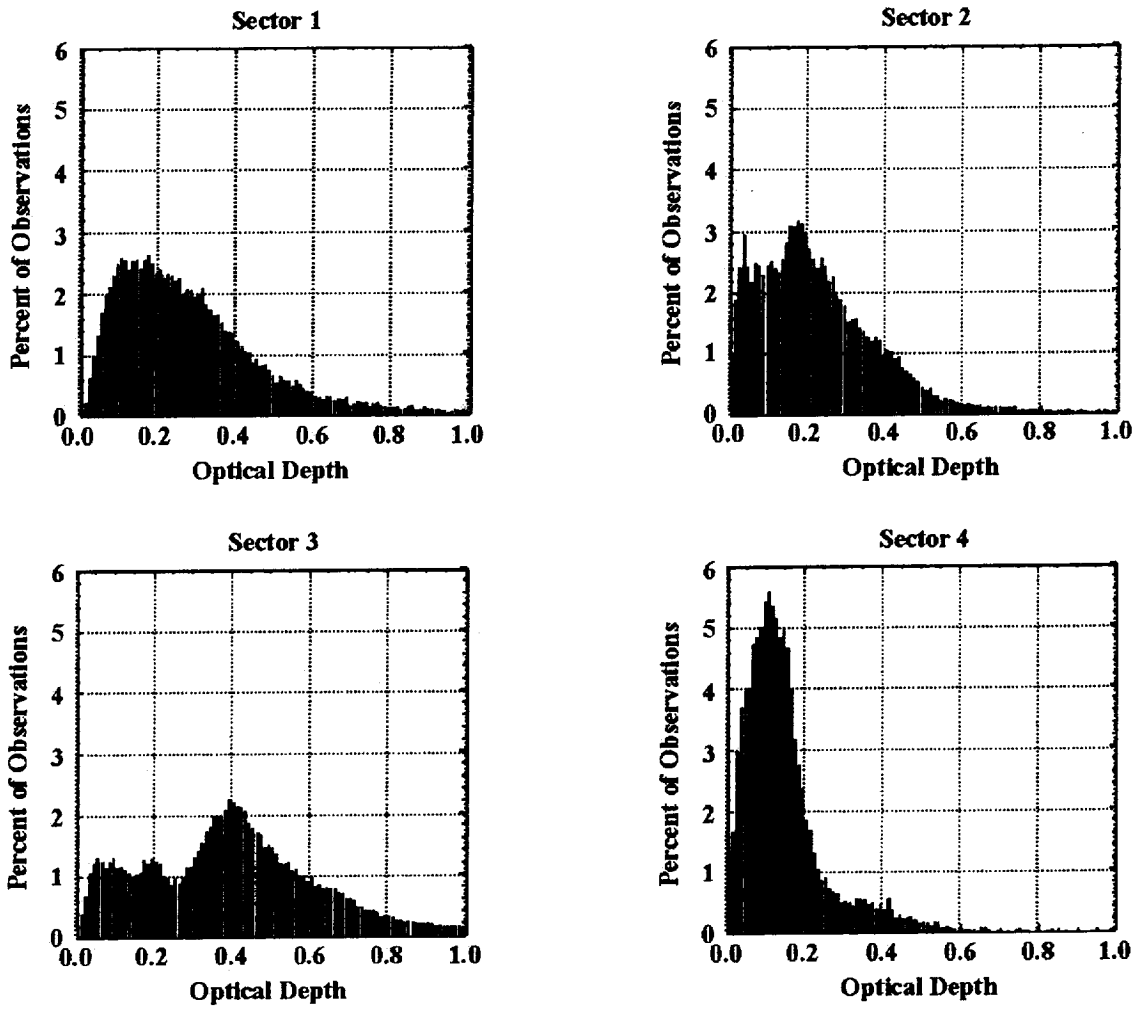

Figure 3: Histograms of 532 nm PBL aerosol optical depth by sector as a percentage of total observations. Sector numbers correspond to those defined in Figures 1 and 2. Optical depth measurements are binned in 0.01 increments.

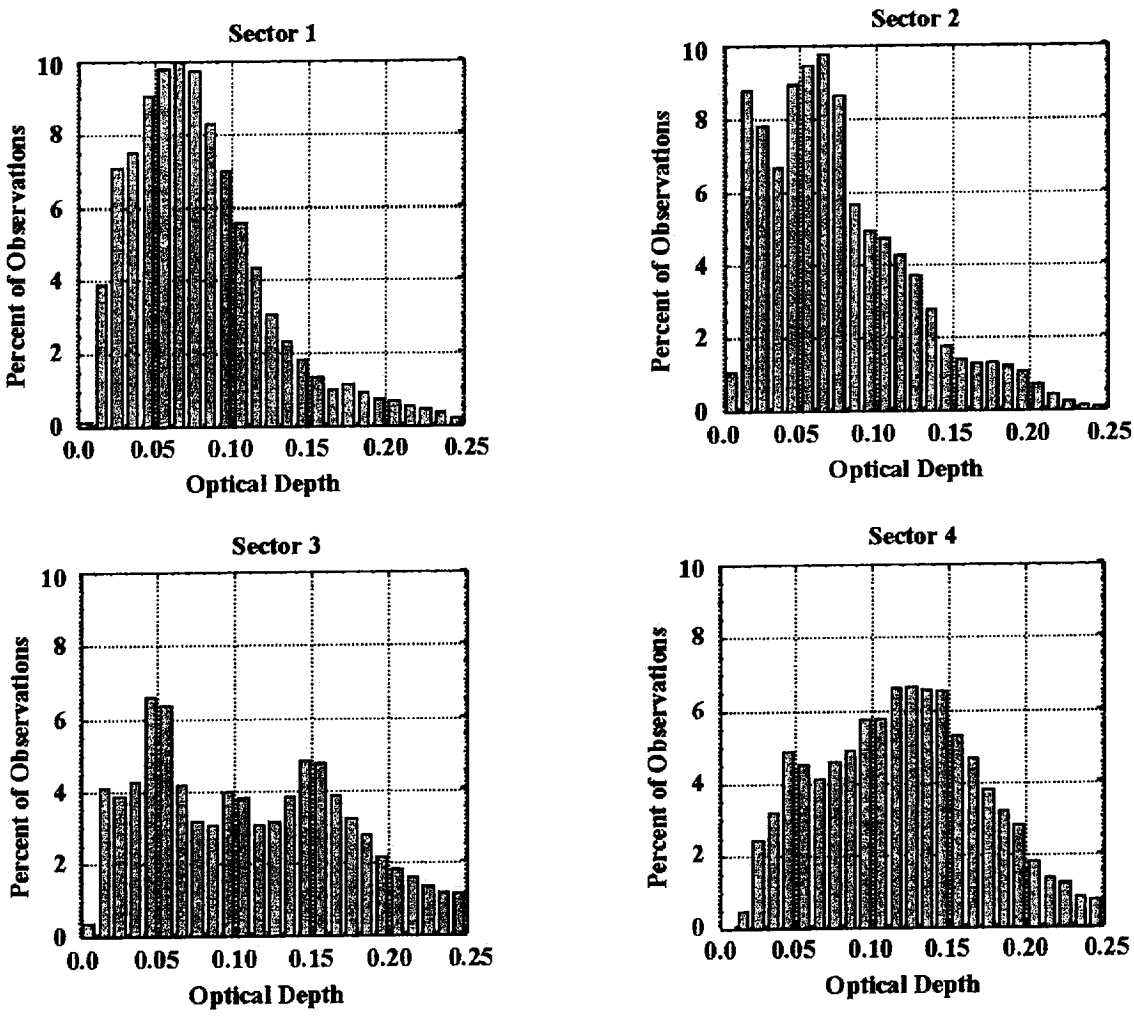

Figure 4: Same as Figure 3, except for 1064 nm PBL aerosol optical depth.

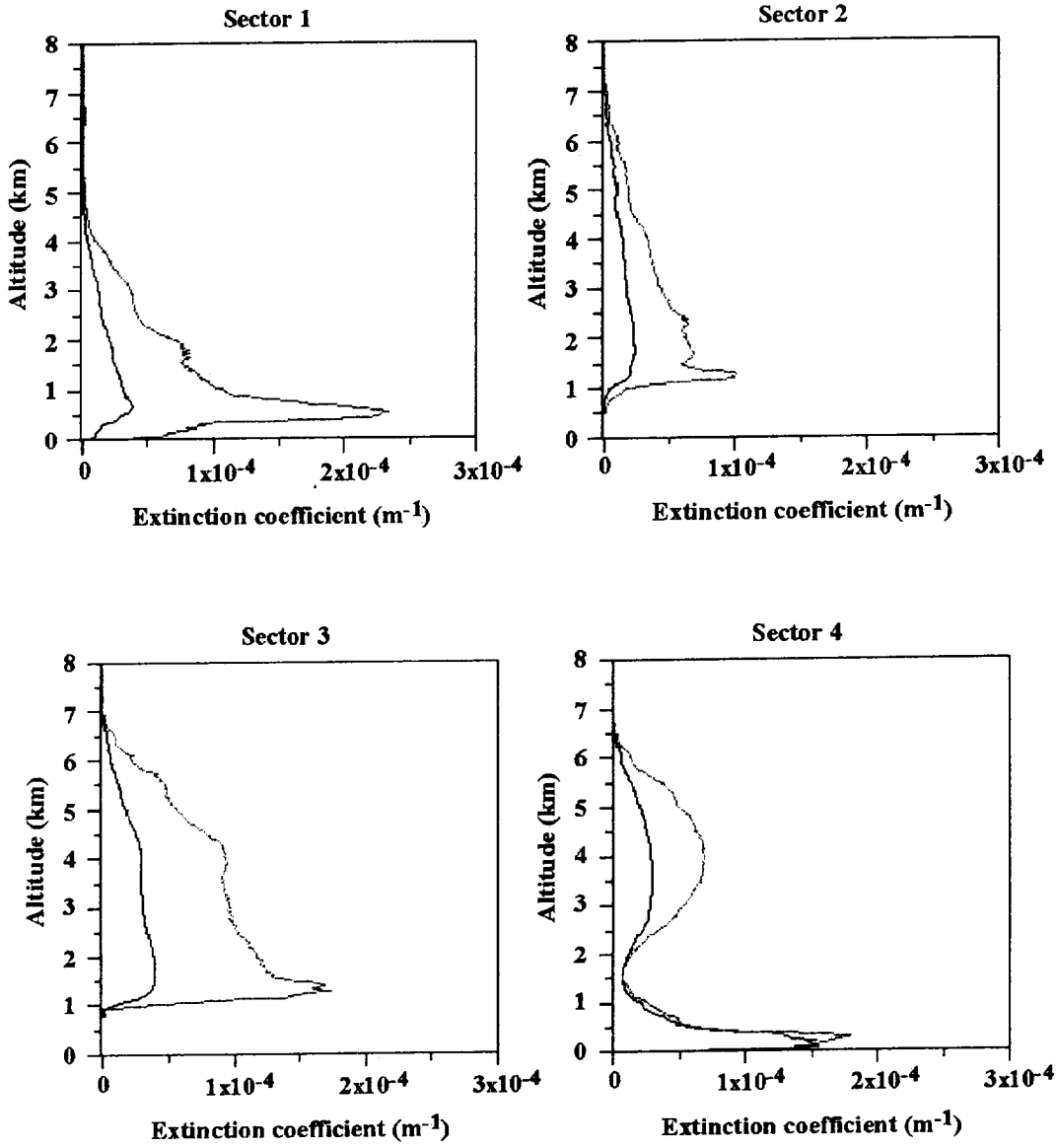

Figure 5: Average profiles of aerosol extinction by sector. Sector numbers correspond to those defined in Figures 1 and 2. In each panel the black line is 1064 nm extinction and the gray line is 532 nm extinction. Only profiles with no cloud contamination are included in the averages. The ground elevation in sectors 2 and 3 was generally ~1 km.

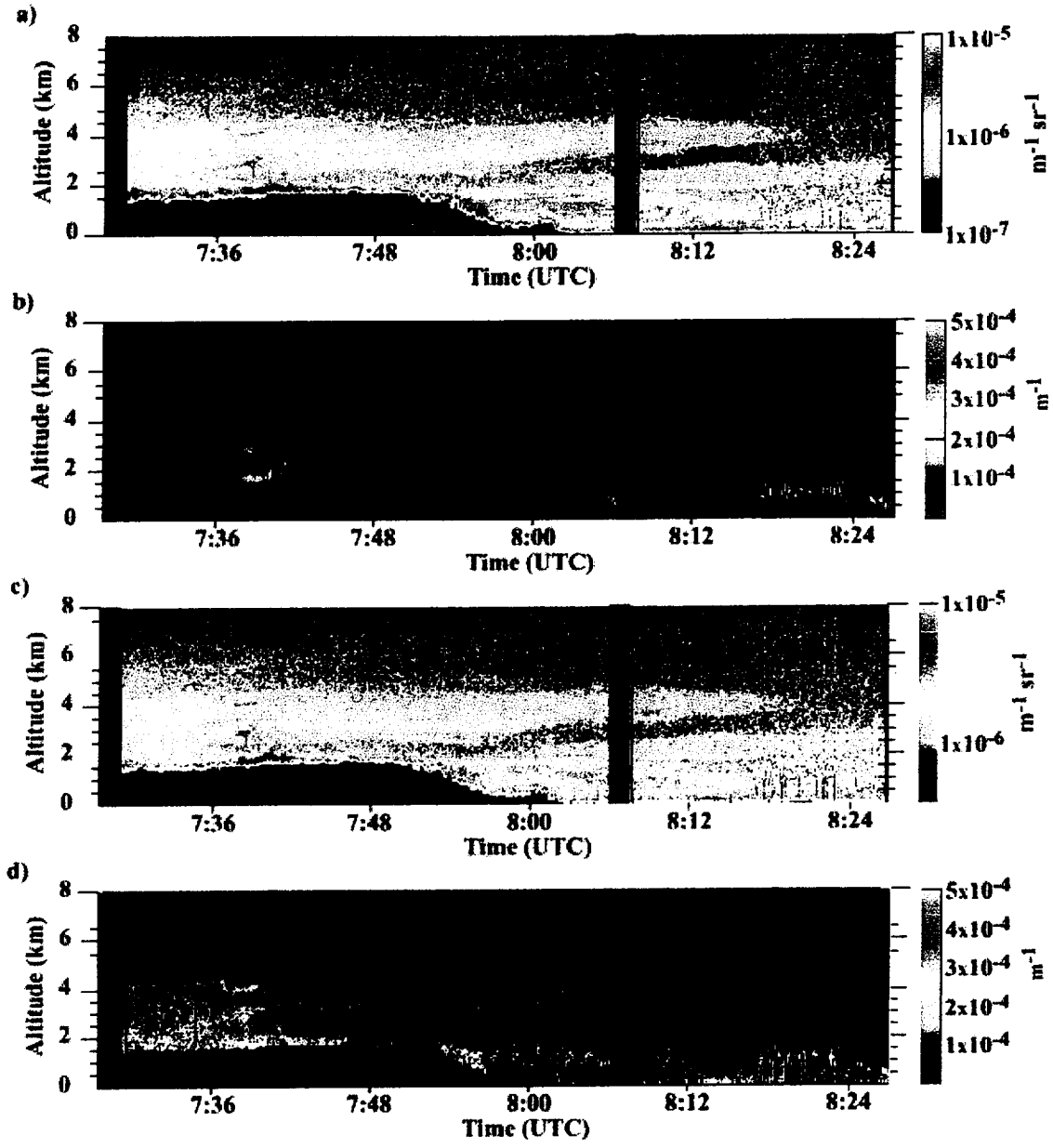

Figure 6: CPL data segment from August 24, 2000 showing elevated aerosol layer above west coast over Inhaca Island. (a) 1064 nm attenuated backscatter profiles; (b) 1064 nm extinction profiles; (c) 532 nm attenuated backscatter profiles; and (d) 532 nm extinction profiles.

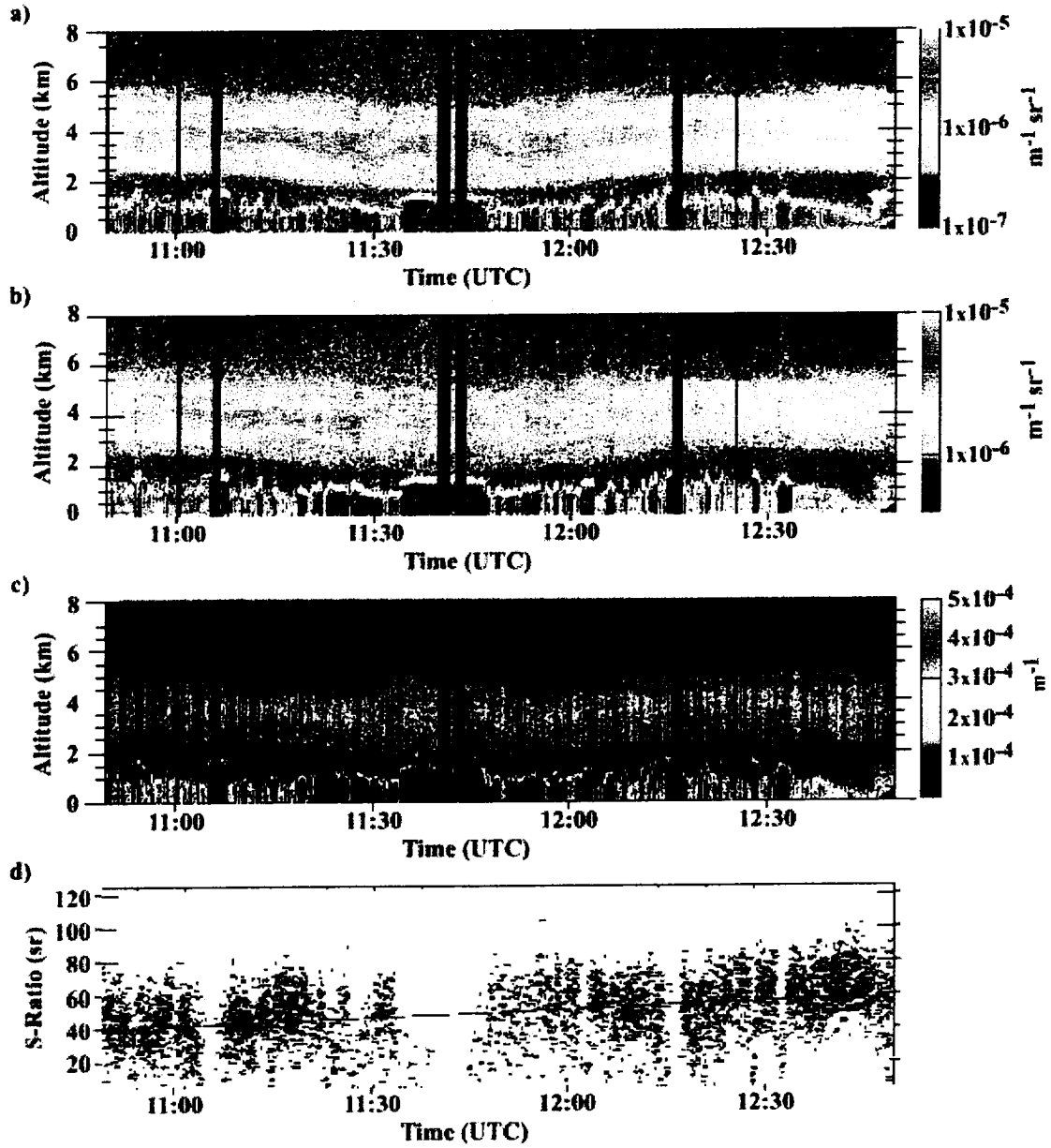

Figure 7: Two-hour data segment from September 14, 2000 showing elevated aerosol layer off the west coast of Namibia. (a) 1064 nm attenuated backscatter profiles; (b) 532 nm attenuated backscatter profiles; (c) 532 nm extinction profiles; and (d) S-ratio of elevated aerosol layer derived from 532 nm data.

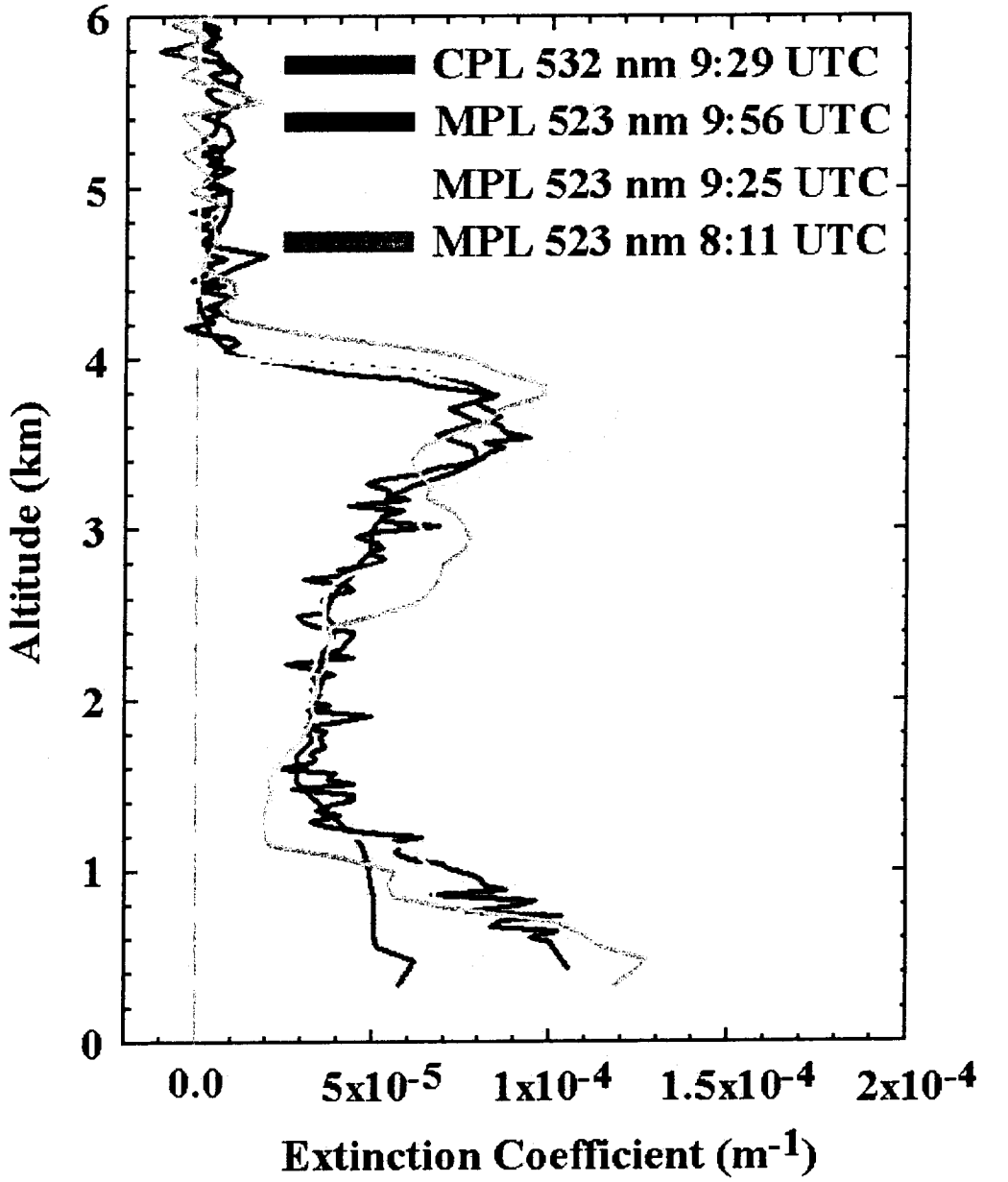

Figure 8: Comparison of extinction profiles from CPL and MPL on August 29, 2000 at Skukuza. CPL profile is a 30-second average. MPL profiles are 30-minute averages centered at the times listed. Differences in the lowest km are due to aerosol inhomogeneity during the measurements.

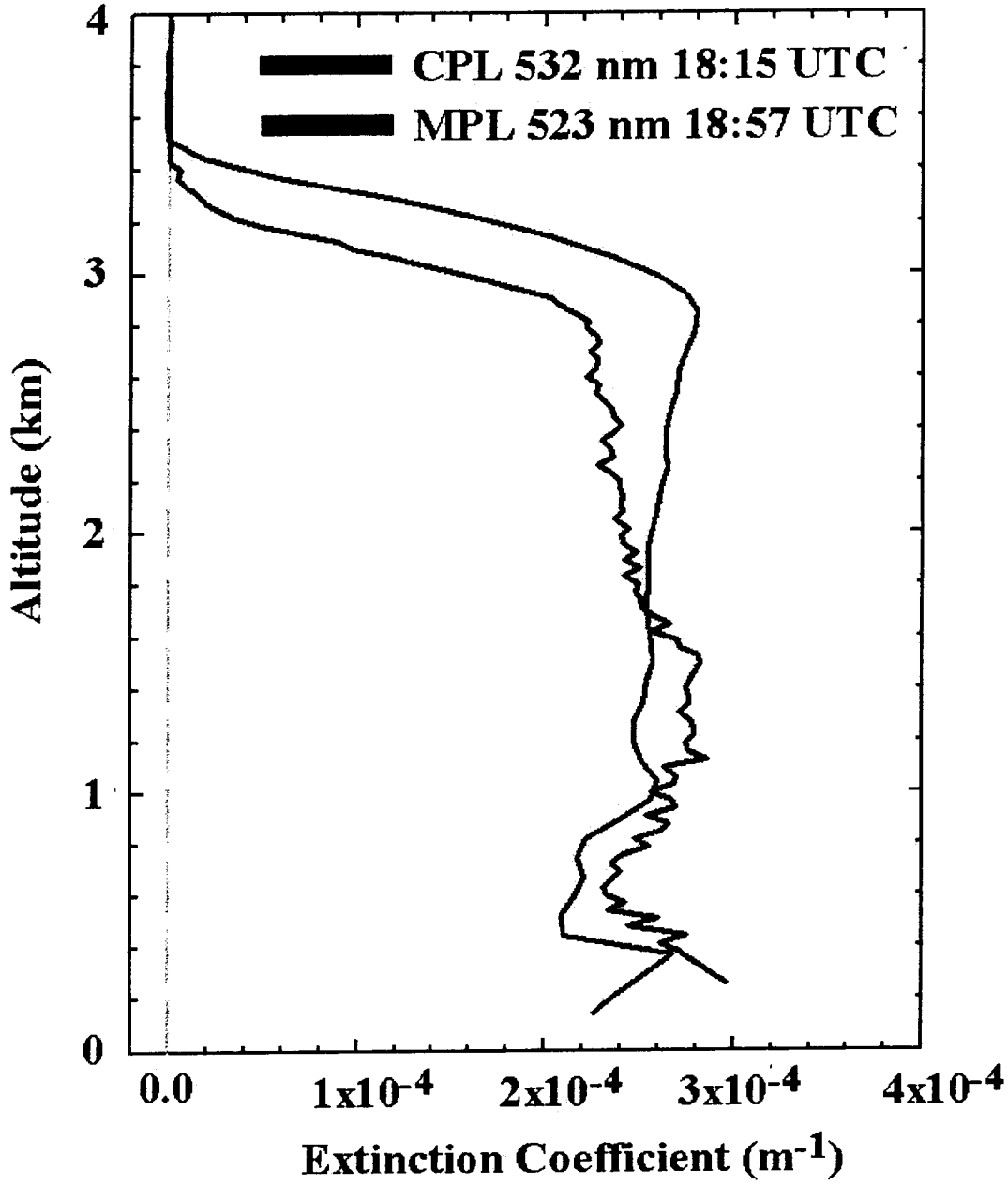

Figure 9: Comparison of extinction profiles from CPL and MPL on September 1, 2000 at Mongu, Zambia. Note difference in magnitude and vertical structure compared to Figure 8.